



## Improved geopolymerization of bottom ash by incorporating fly ash and using waste gypsum as additive

Kornkanok Boonserm<sup>a</sup>, Vanchai Sata<sup>a</sup>, Kedsarin Pimraksa<sup>b</sup>, Prinya Chindaprasirt<sup>a,\*</sup>

<sup>a</sup> Sustainable Infrastructure Research and Development Center, Department of Civil Engineering, Faculty of Engineering, Khon Kaen University, Khon Kaen 40002, Thailand

<sup>b</sup> Department of Industrial Chemistry, Faculty of Science, Chiang Mai University, Chiang Mai 50200, Thailand

### ARTICLE INFO

#### Article history:

Received 27 December 2011

Received in revised form 29 March 2012

Accepted 1 April 2012

Available online 10 April 2012

#### Keywords:

Geopolymer

Flue gas desulfurization gypsum

Bottom ash

Fly ash

Microstructure

Compressive strength

### ABSTRACT

This research studied the improvement of the geopolymerization of bottom ash (BA) by incorporating fly ash (FA) and using flue gas desulfurization gypsum (FGDG) as additive. The BA:FA ratios of 100:0, 75:25, 50:50, 25:75, and 0:100 were used as the blended source materials. The source materials were then replaced with 0%, 5%, 10%, and 15% of FGDG. NaOH, sodium silicate and temperature curing were used to activate the geopolymer. Test results indicated that the increase in FA content in the BA–FA blends improved the strengths of geopolymer mortars owing to the high glassy phase content and high reactivity of FA compared to those of BA. The use of up to 10% of FGDG as additive also significantly increased the strengths of geopolymer. In this case, the compressive strength enhancement was due to the increase in the  $Al^{3+}$  leached from BA in the presence of  $SO_4^{2-}$  and the formation of additional calcium silicate hydrate.

© 2012 Elsevier Ltd. All rights reserved.

### 1. Introduction

Geopolymer is an alkali-activated aluminosilicate cementitious material with a much smaller CO<sub>2</sub> footprint than traditional Portland cement [1]. Several researches have shown that it possesses good strength and mechanical properties [2]. Geopolymerization process relies on the reaction of silica and alumina with high alkali solution. The source materials can, therefore, be industrial or agricultural by-products and solid waste containing silica and/or alumina.

The use of bottom ash (BA) for making alternative cementitious material can both reduce the growth of Portland cement usage and help solve the problem of waste discard at landfill site. BA can also be used as replacement for sand in mortar and concrete [3]. Mae Moh power plant in northern Thailand produces around 0.8 million tons of pulverized coal combustion (PCC) BA per year. Ground to a proper fineness, this BA can be used as source material for making geopolymer with reasonable strength [4]. Research has also shown that the strength of BA geopolymer was lower than that of FA geopolymer [5]. The physical differences such as morphology, particle size, surface properties, and amorphous phase content affect their abilities to react in geopolymer syntheses [6]. For instance, FA is composed of spherical shape and contains high content of amorphous phase which can greatly improve the compressive strength

of geopolymer. In contrast, BA comprises of large fragments with only a small amount of semi-spherical particles [7] and less glassy constituent phase [8].

FA is a good pozzolan and is widely used to replace Portland cement to improve the properties of concrete [9,10]. Both PCC class C and class F fly ashes are good source materials for producing geopolymer [11,12]. To improve the reactivity of low grade source material such as fluidized bed combustion ashes, it is blended with a good source of silica and alumina such as PCC FA and metakaolin [13,14]. The PCC FA is able to increase the workability of the blended ash mixes, contribute to the packing of the source material and thus enhances the strength of the geopolymer products [13].

In the process of burning of coal to generate electricity, many power plants need to reduce the amount of sulfur emission to the atmosphere. The method of desulfurization results in waste material called flue gas desulfurization gypsum (FGDG) in the form of calcium sulfate. Up to now, this waste gypsum has not been utilized and has been discarded at landfill site. It is known that the incorporation of gypsum alters the performances of the Portland cement concrete. Similarly in geopolymer, the addition of gypsum can enhance the degree of geopolymerization [15]. The leaching of alumina can be improved with the presence of sulfate and thus leads to the strength enhancement [16].

The present work aims to improve the strength development of BA geopolymer mortars with the addition of PCC FA and the use of FGDG as additive. This knowledge would be beneficial to the utilization of these waste materials.

\* Corresponding author. Tel.: +66 4320 2355; fax: +66 4320 2355x12.

E-mail address: [prinya@kku.ac.th](mailto:prinya@kku.ac.th) (P. Chindaprasirt).

## 2. Materials and methods

### 2.1. Materials

PCC FA, PCC BA and FGDG from Mae Moh Power Plant in northern Thailand were used. BA was ground and used as the main source material for making geopolymer. The as-received FA was used to replace part of BA to improve the quality of the main source material. FGDG was oven dried at 105 °C, ground and used as additive to improve the strength of the geopolymer. The chemical and mineralogical compositions of FA, BA and FGDG are shown in Table 1. The major oxides of BA and FA were SiO<sub>2</sub>, Al<sub>2</sub>O<sub>3</sub>, Fe<sub>2</sub>O<sub>3</sub>, and CaO with a small SO<sub>3</sub> content. The main compositions of FGDG were CaO and SO<sub>3</sub> oxides. The physical characteristics of materials are shown in Table 2. The median particle sizes of BA, FA, and FGDG were 32.2, 63.5, and 10.3 μ, the percentages retained on No. 325 sieve were 33, 50 and 3 and the specific gravity were 2.86, 2.52, and 2.39, respectively. Sodium hydroxide solution (NaOH) at 10 M concentration and sodium silicate solution (NS) with 13.8% Na<sub>2</sub>O, 32.2% SiO<sub>2</sub>, and 54.0% H<sub>2</sub>O by weight were used as alkali activators. The local river sand with specific gravity of 2.62 and fineness modulus of 2.85 in saturated surface dry condition was used for making geopolymer mortars. The XRD patterns of BA and FA are shown in Fig. 1. Both of BA and FA contained glassy phase and some crystalline phases of quartz (Q: SiO<sub>2</sub>), calcium oxide (C: CaO), and hematite (H: Fe<sub>2</sub>O<sub>3</sub>). The phases of mullite (M: Al<sub>6</sub>Si<sub>2</sub>O<sub>13</sub>) and anhydrite (A: CaSO<sub>4</sub>) were only found in FA, while anorthite (N: CaAl<sub>2</sub>Si<sub>2</sub>O<sub>8</sub>) and augite (U: (Ca(Mg,Al)(Si<sub>2</sub>,Al)O<sub>6</sub>)) were found in BA. The broad hump around 26° (2θ) of BA was smaller than that of FA indicating that the glassy phase of BA was lower than that of FA.

### 2.2. Details of mixes and tests

The NS/NaOH ratio of 1.0, liquid/ash (L/A) ratio of 0.6 and ash/sand ratio of 2.75 were used for making geopolymer. BA was replaced with FA to obtain the blended source materials with BA:FA ratios of 0:100, 25:75, 50:50, 75:25, and 100:0. The blended ashes were replaced with 0%, 5%, 10%, and 15% of FGDG by weight. Table 3 gives the details of mix proportions and molar oxide ratios. The SiO<sub>2</sub>/Al<sub>2</sub>O<sub>3</sub>, Na<sub>2</sub>O/SiO<sub>2</sub> and H<sub>2</sub>O/Na<sub>2</sub>O ratios were 4.56–4.76, 0.30–0.35 and 9.0–10.0, respectively which are comparable to the optimum values of SiO<sub>2</sub>/Al<sub>2</sub>O<sub>3</sub> = 3.0, Na<sub>2</sub>O/SiO<sub>2</sub> = 0.3 and H<sub>2</sub>O/Na<sub>2</sub>O = 10.0 for metakaolin geopolymers [17].

The samples were prepared by mixing BA, FA, and FGDG until the uniform color was obtained. The NaOH was then added and mixed for 5 min. The NS solution was added and mixed for another 5 min. (For geopolymer mortar, sand was then added and mixed again for 5 more minutes). After mixing, the fresh paste or mortar

**Table 2**

Physical characteristics of BA, FA and FGDG.

Materials	Median particles size (μ)	Specific gravity	Retained on sieve #325%
BA	32.2	2.86	33
FA	63.5	2.52	50
FGDG	10.3	2.39	3

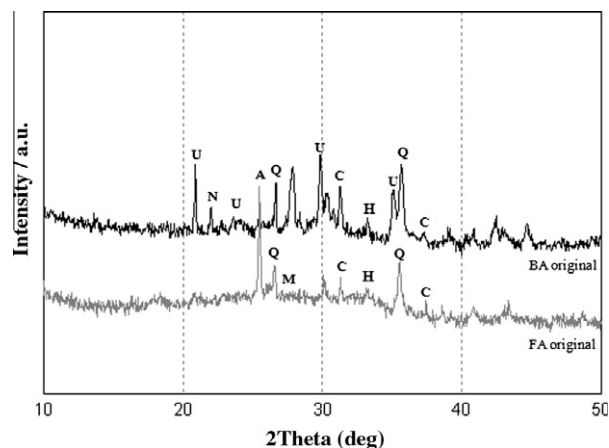


**Fig. 1.** XRD patterns of BA and FA original.

was casted into plastic 5 × 5 × 5 cm cubic molds in accordance with ASTM C109 [18] and subjected to final vibration of 10 s. The molds were then wrapped with polyvinyl sheet to prevent a loss of moisture. Samples were cured in an electric oven at 40 °C for 48 h and then kept at 25 °C and 50% R.H. room. At the age of 7 days, the mortar samples were tested for compressive strengths in accordance with ASTM C109. The paste samples at 28 days were used for the investigations of microstructures. The fractured surfaces were coated with gold and scanned using JEOL scanning electron microscope (SEM). The pastes were ground to particle size less than 75 μ (passed sieve No. 200) and used for XRD analysis using PANalytical X-ray diffractometer with CuKα radiation and fourier transform infrared spectroscopy (FT-IR) at the range of 4000–400 cm<sup>−1</sup>.

## 3. Results and discussion

### 3.1. Compressive strength

The compressive strengths of BA and FA geopolymer mortars with different FGDG contents are shown in Fig. 2. Without FGDG,

**Table 1**

Chemical and mineralogical compositions of BA, FA and FGDG.

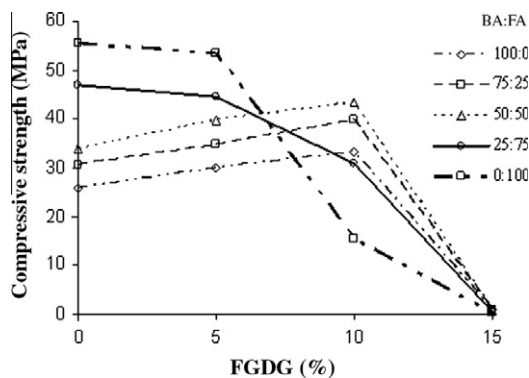
Chemical Composition (%)	Raw materials		
	BA	FA	FGDG
CaO	13.0	24.5	37.7
SiO <sub>2</sub>	35.5	35.2	4.0
Al <sub>2</sub> O <sub>3</sub>	16.8	16.5	2.0
Fe <sub>2</sub> O <sub>3</sub>	15.1	13.6	0.5
SO <sub>3</sub>	0.6	1.6	54.1
Na <sub>2</sub> O	3.8	2.7	0.0
MgO	8.4	3.2	1.6
K <sub>2</sub> O	1.8	1.9	0.1
P <sub>2</sub> O <sub>5</sub>	0.2	0.2	0.0
TiO <sub>2</sub>	0.3	0.3	0.0
Loss on ignition	4.7	0.4	14.7
Mineral composition	Quartz, anorthite, augite, magnetite, mullite	Anhydrite, quartz, magnetite, calcium oxide, mullite	Gypsum

**Table 3**

Mix proportions of BA and/or FA geopolymer with FGDG.

Series	BA:FA	FGDG (%)	SiO <sub>2</sub> /Al <sub>2</sub> O <sub>3</sub>	Na <sub>2</sub> O/ SiO <sub>2</sub>	H <sub>2</sub> O/ Na <sub>2</sub> O	Ms
A	100:0	0	4.56	0.32	9.00	3.11
		5	4.61	0.33	9.11	3.04
		10	4.65	0.34	9.23	2.97
		15	4.71	0.35	9.35	2.90
B	75:25	0	4.57	0.32	9.16	3.16
		5	4.62	0.32	9.28	3.09
		10	4.67	0.33	9.39	3.01
		15	4.72	0.34	9.51	2.94
C	50:50	0	4.59	0.31	9.34	3.22
		5	4.63	0.32	9.45	3.14
		10	4.68	0.33	9.55	3.06
		15	4.73	0.34	9.67	2.98
D	25:75	0	4.60	0.31	9.52	3.28
		5	4.64	0.31	9.62	3.19
		10	4.69	0.32	9.72	3.11
		15	4.75	0.33	9.83	3.03
E	0:100	0	4.61	0.30	9.71	3.33
		5	4.66	0.31	9.80	3.25
		10	4.71	0.32	9.90	3.16
		15	4.76	0.33	10.00	3.08

Note: water/solid = 0.30.

**Fig. 2.** Compressive strength of BA and FA geopolymer mortars with 0–15% FGDG.

the compressive strengths of pure BA and FA geopolymer mortars were 25.5 and 55.5 MPa, respectively. The degree of geopolymerization of the FA geopolymer is higher than that of the BA geopolymer [5] owing to the high glassy phase content and higher reactivity of FA compared to those of BA. Additionally, Ca<sup>2+</sup> reacted with silicate from FA and formed additional calcium silicate hydrate (CSH) gel [15,19]. The strength of blended geopolymer mortars, therefore, improved with the increase in the FA content. For the low FA content of 0%, 25%, and 50%, the strengths of geopolymer mortars were reasonable at 25.5, 30.5, and 34.0 MPa, respectively. The addition of 5–10% of FGDG significantly increased the compressive strengths of mortars. For example, the strength of 75:25 (BA:FA) blend replaced with 0%, 5%, and 10% FGDG mortars were 30.5, 35.0, and 40.0 MPa. The strength enhancement was due to the increased Ca<sup>2+</sup> reacted with silicate and formed additional CSH and also reacted with aluminosilicate group and strengthened the aluminosilicate network [20]. In addition, SO<sub>4</sub><sup>2-</sup> ions in the system promoted the dissolution of Al<sup>3+</sup> ions in BA [21] and led to a stronger geopolymer.

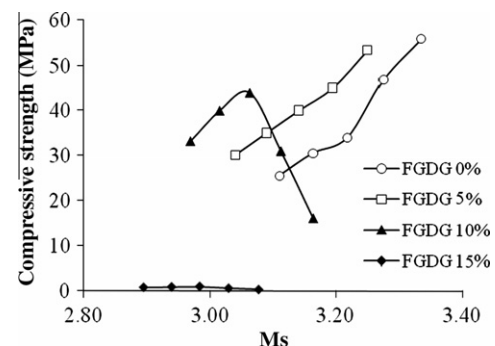
When the FGDG content was increased to 15%, the strengths of all mortar mixes were very low between 0.3 and 1.0 MPa. The high FGDG content obstructed the geopolymerization process and drastically reduced the strength of the mortar. Also for the high FA content of 75% and 100% where the strength of mortars were already high, the incorporation of FGDG decreased the strength of mortars.

The reduction was dependent on the replacement level. At low replacement level of 5% of FGDG, the strengths were slightly reduced. The strength reductions were significant when the replacement levels were 10% and 15%. For the high FA blended mixture, the dissolution of the Si and Al ions was already in a good state and hence the addition of FGDG did not enhance the dissolution of Al ions.

In normal geopolymer system, the molar SiO<sub>2</sub>/Na<sub>2</sub>O ratios or Ms has a significant effect on strength [22]. The Ms values and strengths of geopolymer mortars were, therefore, plotted as shown in Fig. 3. At low 0% and 5% FGDG, the compressive strengths increased with Ms as expected. At the low dosage level, the effect of FGDG on strength was not large. For 10% FGDG, the trend of compressive strength versus Ms started to change. This was probably due to the increase in effect of FGDG. The mortars with high BA content still exhibited the normal increase in strength with the increase in Ms. For mortars with high FA content, however, the strengths reduced with the increase in Ms indicating the negative effect of FGDG. For high FGDG addition of 15%, the negative effect of FGDG became dominant and the compressive strengths of all mixes were adversely affected.

### 3.2. Scanning electron microscope

The SEM-photomicrographs of BA and FA geopolymer pastes with different FGDG contents as shown in Fig. 4 indicated that

**Fig. 3.** Compressive strength and Ms of BA and FA geopolymer mortars with 0–15% FGDG.

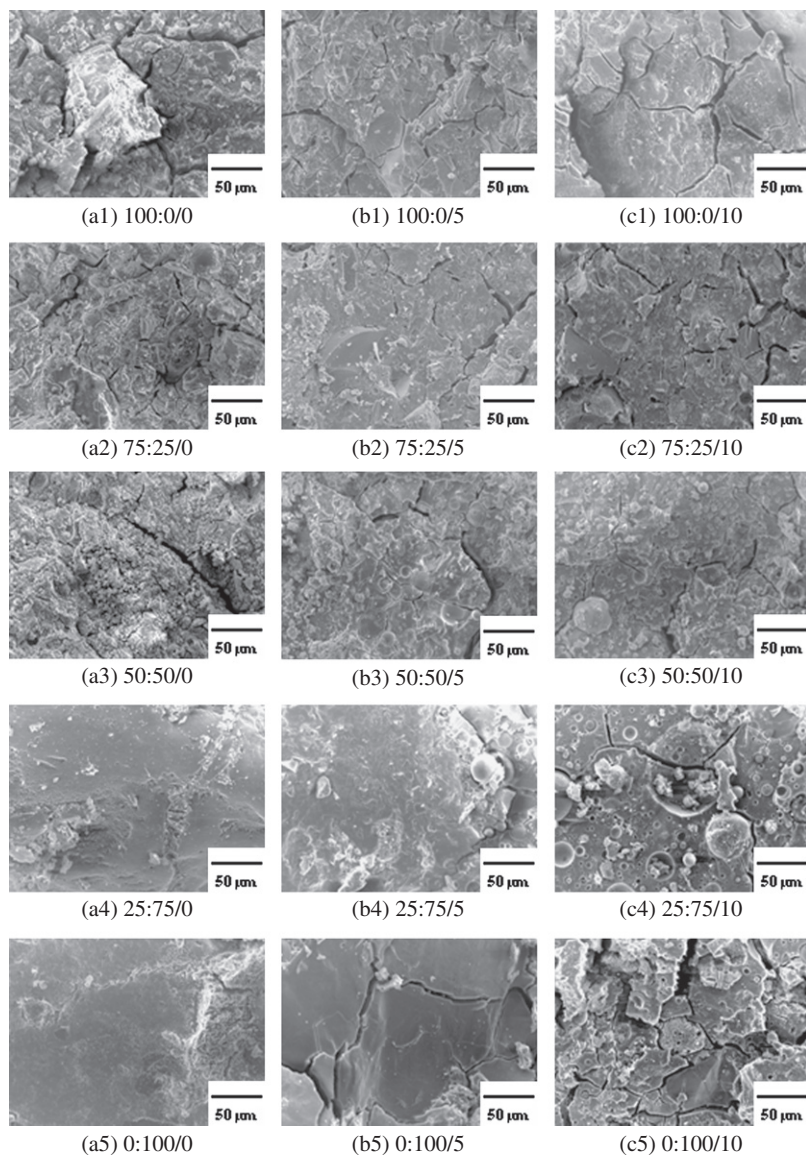


Fig. 4. SEM photography of fractured BA and FA geopolymer pastes (BA:FA/FGDG).

the polymerization products were well-connected structures consisting of glassy phase structures with no definite grain boundary. Without FG DG, the matrices of high FA content geopolymer (mixes with 75% and 100% FA) appeared very dense as shown in Fig. 4a4 and a5. For the mixes with 0%, 25%, and 50% FA, the matrices were less dense and less homogenous as shown in Fig. 4a1–a3. For the low FA mixes (mixes with 0% and 25% FA), the incorporation of 5% and 10% FG DG appeared to improve the homogeneity and the denseness of the matrices as shown in Fig. 4a1–c1 and a2–c2. The principle of activation by FG DG is based on the ability of the sulfate ions to react with alumina in ashes led to the dense aluminosilicate network [23]. For high FA mixes, the incorporation of 10% FG DG appeared to lower the homogeneity and the denseness of the matrices as shown in Fig. 4c4 and c5. The samples with good homogeneity and dense matrix corresponded to mixes with high compressive strengths.

In order to check the Si/Al ratios of the geopolymer products, the EDX study was performed on the FA and BA geopolymer pastes. The results are shown in Table 4. With no FG DG, the geopolymer products of 100% FA and 100% BA mixes contained average Si/Al

Table 4

The Si/Al ratios of BA and/or FA geopolymer pastes with FG DG calculated from EDX.

Series	BA:FA	FG DG (%)	Si/Al ratios
A	100:0	0	5.41
		5	4.43
		10	3.76
E	0:100	0	2.93
		5	3.09
		10	3.33

ratios of 2.93 and 5.41, respectively. The high Si/Al ratio gave geopolymer with low strength but good elasticity properties [24]. The dissolution of Al ions from aluminosilicate glassy phases of FA was much easier than that of BA even though the  $\text{Al}_2\text{O}_3$  contents of both FA and BA were similar. Furthermore, the Si/Al ratios of FA geopolymer increased, while those of BA geopolymer reduced with the addition of FG DG as shown in Table 4. The dissolution of Al from FA was obstructed, while the dissolution of Al from BA geopolymer was enhanced with the presence of sulfate ions.



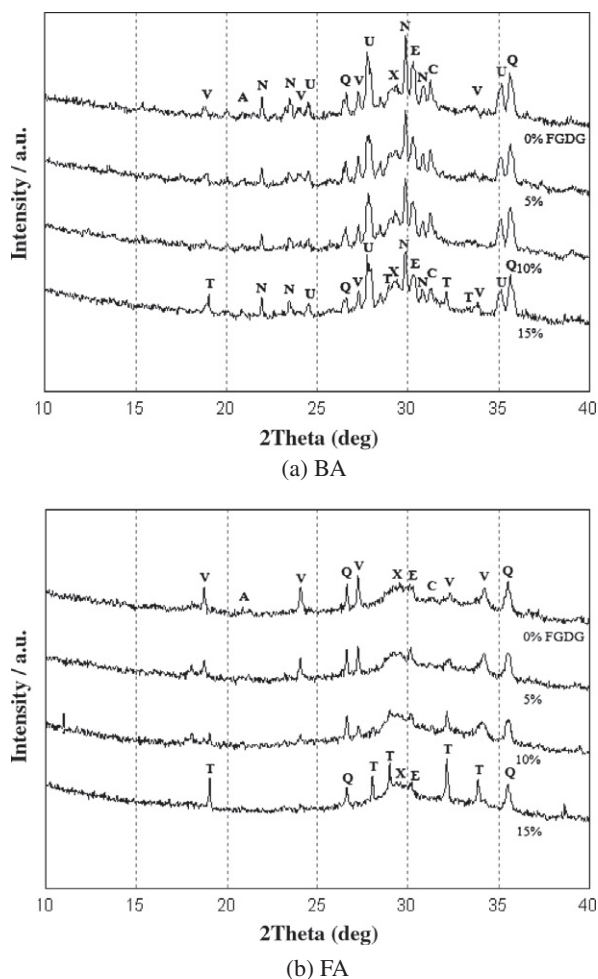


Fig. 5. XRD patterns of BA and FA geopolymer pastes with 0–15% FGDG.

### 3.3. X-ray diffraction

The XRD patterns of BA and FA geopolymer pastes are shown in Fig. 5. In general, the XRD patterns of the source materials and those of the BA and FA geopolymers were not very different. For BA and FA geopolymer pastes, the intensity peaks of  $\text{SiO}_2$  (Q) and

CaO (C) reduced, while CSH (X), amorphous phase, and aluminosilicate gel around  $30^\circ$  ( $2\theta$ ) increased as compared to those of the source materials. Additionally, gehlenite (E:  $\text{Ca}_2\text{Al}_2\text{SiO}_7$ ) phase and the new zeolite phases named vishnevite (V:  $\text{Na}_8\text{Al}_6\text{Si}_6\text{O}_{24}(\text{SO}_4)\cdot 2\text{H}_2\text{O}$ ) and thenardite (T:  $\text{Na}_2\text{SO}_4$ ) were presented in both geopolymers.

For BA geopolymer, the phases were transformed into more stable known as anorthite and augite aluminum. The addition of 5–10% FGDG in BA produced the additional increases in CSH, gehlenite, and vishnevite phases. The strength enhancement was due to the presence of some of these crystalline phases [25,26]. The increase of FGDG to 15% produced thenardite ( $\text{Na}_2\text{SO}_4$ ) phase which did not contribute to the strength of geopolymer.

For FA geopolymer, the results showed the increases in CSH, vishnevite, and glassy phase compared to BA geopolymer. The incorporation of 5–15% FGDG resulted in an increase in the thenardite phase but a decrease in the vishnevite phase. The large percentage of thenardite phase existed as an impurity in the system [27] and thus weakened the geopolymer.

### 3.4. IR spectra

The results of the IR spectra of BA and FA source materials and BA and FA geopolymer pastes are shown in Fig. 6. The considerable broad bands located at  $3700\text{--}2200\text{ cm}^{-1}$  and  $1700\text{--}1600\text{ cm}^{-1}$  were assigned to O–H stretching and H–O–H bending, respectively. These characterized the spectrum of stretching and deformation vibration of O–H and H–O–H groups from the weakly bound water molecules which were adsorbed on the surface or trapped in large cavities between the rings of geopolymer products [28]. The increase in  $\text{H}_2\text{O}/\text{Na}_2\text{O}$  mole ratios (Table 3) raised the intensity of peaks at  $3500$  and  $1650\text{ cm}^{-1}$ . The Si–O–Si and Al–O–Si stretching vibrations related to the degree of geopolymerization were detected at the wave number of  $950\text{ cm}^{-1}$ . The increases in FA and FGDG provided high intensity Si–O–Si and Al–O–Si bands. The spectra at  $1460\text{ cm}^{-1}$  represented the sodium carbonate from carbonation process which resulted from the unreacted  $\text{Na}_2\text{O}$  [17].

The addition of FGDG resulted in a noticeable change in the spectra of BA and FA geopolymer pastes. The  $\text{SO}_4^{2-}$  bonding was detected at wave numbers of  $1200$  and  $636\text{ cm}^{-1}$  for S=O stretching and  $\text{Na}_2\text{SO}_4$ , respectively [29]. This demonstrated that  $\text{SO}_4^{2-}$  ion reacted with alkaline solution and formed  $\text{SO}_4$  compound. For BA geopolymer,  $\text{SO}_4$  compound could not be detected with the

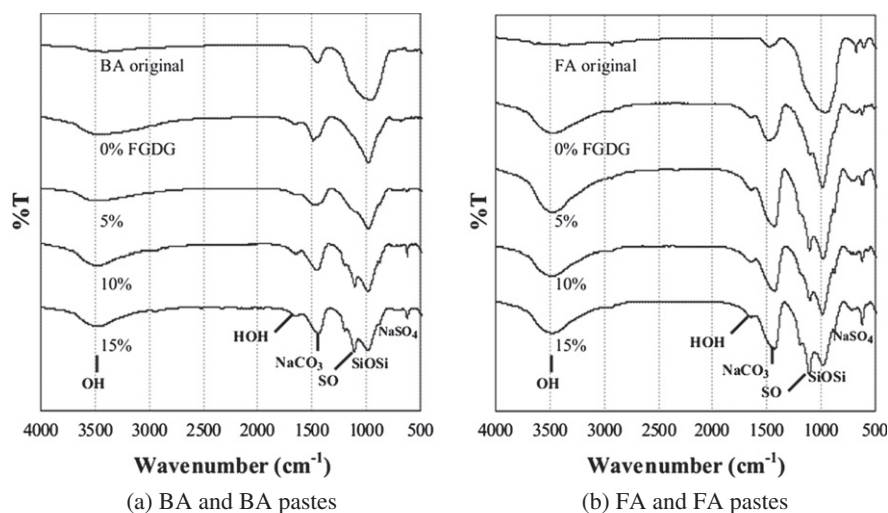


Fig. 6. FTIR of BA, FA and BA and FA geopolymer pastes with 0–15% FGDG.

addition of low FGDG content of 5%. The presences of  $\text{SO}_4$  compound were noticeable at 10% and 15% FGDG addition. At high FGDG content of 15%, the  $\text{SO}_4$  compounds were clearly observed. The presence of  $\text{SO}_4$  compounds in large quantity was related to the very low strength of geopolymer mortars. For FA geopolymer, the presence of  $\text{SO}_4$  compound was noticeable with the addition of only 5% FGDG. At the high 10 and 15% FGDG, the peaks at 1200 and  $636\text{ cm}^{-1}$  were quite distinctive. This caused the low strengths of FA geopolymer mortars containing FGDG.

#### 4. Conclusions

The results demonstrated that the geopolymerization of BA was enhanced with the blending with FA and the addition of 5% FGDG. The strength of BA geopolymer mortar was lower than that of FA mortar. FA contained a higher amount of glassy phase and was more reactive than BA. The blending of BA with FA, therefore, increased the strength of the BA geopolymer mortars. The incorporation of 5% FGDG also resulted in the strength improvement of BA geopolymer mortar. The presence of sulfate ions increased the dissolution of Al ions from the BA and thus enhanced the geopolymerization and strength of the BA geopolymer. The incorporation of 10 and 15% of FGDG resulted in the thenardite phase which existed as an impurity in the system and weakened the geopolymer.

#### Acknowledgments

This work was supported by the Electricity Generating Authority of Thailand (EGAT), the Thailand Research Fund (TRF) under the TRF Senior Research Scholar, Grant No. RTA5480004, and the Royal Golden Jubilee Ph.D. program Grant No. PHD/0210/2551.

#### References

- [1] Duxson P, Provis JL, Lukey GC, Van Deventer JSJ. The role of inorganic polymer technology in the development of 'green concrete'. *Cem Concr Res* 2007;37(12):1590–7.
- [2] Davidovits J. Properties of geopolymer cements. In: Krivenko PV editor. *Proceedings of the 1st international conference on alkaline cements and concretes*. Ukraine, 1994. p. 131–49.
- [3] Kula I, Olgunb A, Erdoganb Y, Sevinc V. Effects of colemanite waste, coal bottom ash and fly ash on the properties of cement. *Cem Concr Res* 2001;31(3):491–4.
- [4] Sathonsaowaphak A, Chindaprasirt P, Pimraksa K. Workability and strength of lignite bottom ash geopolymer mortar. *J Hazard Mater* 2009;168(1):44–50.
- [5] Chindaprasirt P, Jaturapitakkul C, Chalee W, Rattanasak U. Comparative study on the characteristics of fly ash and bottom ash geopolymers. *Waste Manage* 2009;29(2):539–43.
- [6] Jaturapitakkul C, Cheerarat R. Development of bottom ash as pozzolanic material. *J Mater Civil Eng* 2003;15(1):48–53.
- [7] Hart BR, Powell MA, Fyfe WS, Ratanasthien B. Geochemistry and mineralogy of fly-ash from the Mae Moh lignite deposit, Thailand. *Energy Source* 1995;17(1):23–40.
- [8] Demir I, Hughes RE, DeMaris PJ. Formation and use of coal combustion residues from three types of power plants burning Illinois coals. *Fuel* 2001;80(11):1659–73.
- [9] Olgun A, Atar N, Bütün V, Erdogan Y. Effect of DMA–MMA diblock copolymer on the properties of Portland and composite cement. *Cem Concr Compos* 2008;30(4):334–46.
- [10] Yilmaz B, Olgun A. Studies on cement and mortar containing low-calcium fly ash, limestone, and dolomitic limestone. *Cem Concr Compos* 2008;30(3):194–201.
- [11] Swanepoel JC, Strydom CA. Utilisation of fly ash in geopolymeric material. *Appl Geochem* 2002;17(8):1143–8.
- [12] Chindaprasirt P, Chareerat T, Sirivivatnanon V. Workability and strength of coarse high calcium fly ash geopolymer. *Cem Concr Compos* 2007;29(3):224–9.
- [13] Chindaprasirt P, Rattanasak U. Utilization of blended fluidized bed combustion (FBC) ash and pulverized coal combustion (PCC) fly ash in geopolymer. *Waste Manage* 2010;30(4):667–72.
- [14] Xu H, Li Q, Shen L, Zhang M, Zhai J. Low-reactive circulating fluidized bed combustion (CFBC) fly ashes as source material for geopolymer synthesis. *Waste Manage* 2010;30(1):57–62.
- [15] Rattanasak U, Pankhet K, Chindaprasirt P. Effect of chemical admixtures on properties of high-calcium fly ash geopolymer. *Int J Miner Metall Mater* 2011;18(3):364–9.
- [16] Pimraksa K, Chindaprasirt P. Lightweight bricks made of diatomaceous earth, lime and gypsum. *Ceram Int* 2009;35(1):471–8.
- [17] Barbosa VFF, MacKenzie KJD, Thaumaturgo C. Synthesis and characterisation of materials based on inorganic polymers of alumina and silica: sodium polysialate polymer. *Int J Inorg Mater* 2000;2(4):309–17.
- [18] ASTM C109/C109M-08. Standard test method for compressive strength of hydraulic cement mortars (using 2-in. or [50-mm] cube specimens). American Society for Testing and Materials, Philadelphia; 2008.
- [19] Guo X, Shi H, Dick AW. Compressive strength and microstructural characteristics of class C fly ash geopolymer. *Cem Concr Compos* 2010;32(2):142–7.
- [20] Taiyib J, MacKenzie JKD. Structure and mechanical properties of aluminosilicate geopolymer composites with Portland cement and its constituent minerals. *Cem Concr Res* 2010;40(5):787–94.
- [21] Ma W, Liu C, Brown PW, Komarneni S. Pore structures of fly ashes activated by  $\text{Ca}(\text{OH})_2$  and  $\text{CaSO}_4 \cdot 2\text{H}_2\text{O}$ . *Cem Concr Res* 1995;25(2):417–25.
- [22] Chen JH, Huang JS, Chang YW. Use of reservoir sludge as a partial replacement of metakaolin in the production of geopolymers. *Cem Concr Compos* 2011;33(5):602–10.
- [23] Aimin X, Sarker SL. Microstructural study of gypsum activated fly ash hydration in cement paste. *Cem Concr Res* 1991;21(6):1137–47.
- [24] Fletcher RA, MacKenzie KJD, Nicholson CL, Shimada S. The composition range of aluminosilicate geopolymers. *J Eur Ceram Soc* 2005;25(9):1471–7.
- [25] Álvarez-Ayuso E, Querol X, Plana F, Alastuey A, Moreno N, Izquierdo M, et al. Environmental, physical and structural characterisation of geopolymer matrixes synthesised from coal (co-)combustion fly ashes. *J Hazard Mater* 2008;154(1–3):175–83.
- [26] Rattanasak U, Chindaprasirt P. Influence of NaOH solution on the synthesis of fly ash geopolymer. *Miner Eng* 2009;22(12):1073–8.
- [27] Luke K. The effect of natural zeolites on the composition of cement pore fluids at early ages. In: *Proceedings of 12th international congress on the chemistry of cement*, Halliburton, USA; 2007.
- [28] Palomo A, Grutzeck MW, Blanco MT. Alkali-activated fly ashes: a cement for the future. *Cem Concr Res* 1999;29(8):1323–9.
- [29] Bakharev T. Durability of geopolymer materials in sodium and magnesium sulfate solutions. *Cem Concr Res* 2005;35(6):1233–46.